17.6 Rapid and Energy-Efficient Molecular Sensing Using Dual mm-Wave Combs in 65nm CMOS: A 220-to-320GHz Spectrometer with 5.2mW Radiated Power and 14.6-to-19.5dB Noise Figure

Cheng Wang, Ruonan Han

Massachusetts Institute of Technology, Cambridge, MA

Millimeter-wave/terahertz rotational spectroscopy offers ultra-wide-detection range of gas molecules for chemical and biomedical sensing. Therefore, wideband, energy-efficient, and fast-scanning CMOS spectrometers are in demand. Spectrometers using narrow-pulse sources and electromagnetic scattering [1] are broadband, but their resolutions do not meet the requirement (<10kHz) of the absolute specificity. Alternatively, a scheme using a single tunable tone exhibits significant trade-off between bandwidth and performance. The 245GHz spectrometer in [2] presents 4mW radiated power, but only has a 14GHz bandwidth. In [3] and [4], broader bandwidths are achieved at the expense of degraded radiated power (0.1mW) and noise figure (NF=18.4 to ~23.5dB). In addition, given a typical 10kHz resolution and 1ms integration time, scanning a 100GHz bandwidth with a single tone takes as long as 3 hours. This paper reports a rapid, energy-efficient spectrometer architecture based on dual-frequency-comb scanning. A 220-to-320GHz CMOS spectrometer prototype based on this architecture is demonstrated with a total radiated power of 5.2mW and a NF of 14.6 to ~19.5dB.

The spectrometer shown in Fig. 17.6.1 consists of two identical comb chips with a fixed frequency offset f_{IF}. From each comb, 10 frequency lines are transmitted through the gas sample and are simultaneously used as a local-oscillator (LO) signal for the heterodyne mixing of the wave from another comb. The maximum scanning speed of a single-tone spectrometer with certain sensitivity is determined by the probing signal power, which is fundamentally limited by the population saturation of molecular states. In comparison, in a comb, each probing channel reaches such maximum speed, leading to a much shorter total scanning time through parallel operation. Each comb chip is driven by a tunable reference signal, f_{ref} (45 to 46.67GHz). This signal is tripled to f_0 (135 to 140GHz) and power-divided into up- and down-conversion chains. The chains produce tones evenly spaced every 5GHz using an external clock signal f_D of 10GHz, which is frequency-divided by 2 inside every up/down mixer. Each tone is then doubled and radiated by an active-molecular-probe (AMP) block. The final 10 comb lines located at $6f_{ref}+i\cdot 10$GHz $(i=-5\ldots+4)$ are simultaneously radiated from the chip backside and seamlessly cover 220-to-320GHz band. The proposed comb architecture enables scalability to higher bandwidth with extended cascading of narrowband channels. The narrowband operation also eliminates the aforementioned bandwidth-performance trade-offs in circuits.

In the AMP, the energy efficiency is further improved with multifunctional structures and optimum device feedback. Shown in Fig. 17.6.2, the AMP core serves as a radiating frequency doubler and a subharmonic mixer simultaneously. In the doubler mode, an NMOS pair is driven differentially at f_0. The drain voltage swing is boosted via two $\lambda/4$ resonators, Slot1. At $2f_0$, in-phase standing waves are formed inside Slot1, which acts as a folded slot antenna with a simulated radiation efficiency of 45%. Next, Slot2, which supports the quasi-TEM wave associated with the differential mode at f_0, partially recycles the amplified signal back to the input. When harmonic signal at $2f_0$ is generated at the NMOS drains, the TM wave associated with its common mode is rejected in Slot2. That prevents the leakage of $2f_0$ signal into the lossy gates through the feedback path. The amplitude and phase of the recycled signal at f_0 is controlled by the characteristic impedance and phase of TL1 and Slot2. Shown in Fig. 17.6.2, their optimum values ($Z_{TL1}=30\Omega$, $\theta_{TL1}=55°$, $Z_{Slot2}=80\Omega$, $\theta_{Slot2}=88°$) enable in-phase addition between input and recycled waves without causing instability. Compared to conventional designs without feedback, the simulated doubler conversion efficiency at 275GHz increases from 18% to 43%. In the mixer mode, the input wave at $2f_0+f_{IF}$ is coupled into the heavily driven transistors via the folded slot antenna (Slot1). Both the input signal and the LO signal at $2f_0$ are in common mode, which enable the extraction of the combined, down-converted signal f_{IF} through an integrated RF chock. The simulated single-sideband (SSB) NF is 20.2dB at 275GHz and is improved to 16.3dB when the transistor drain-bias current is zero due to lower thermal and flicker noise.

In these AMPs, phase and amplitude imbalance of baluns (Fig. 17.6.1) deteriorate the efficiency and LO-leakage rejection. Figure 17.5.3 shows an on-chip balun using orthogonal-mode filtering similar to that in Slot2 (Fig. 17.6.2). Only the fully differential quasi-TEM wave is allowed to propagate from the input port to the perfectly symmetric output ports of the balun. This mechanism leads to near-zero imbalance between the two output ports, which is verified by the simulation results in Fig. 17.6.3. Figure 17.6.3 also shows the up/down mixer for comb-spectral generation. Up and down frequency conversions are achieved by selected combination of quadrature signals at f_0 and 5GHz. In simulation, the LO and image rejections are better than 30dB, and the conversion loss is 2.3dB. The 5GHz I/Q signals are generated by a digital frequency divider inside each mixer.

The chip is implemented using a bulk 65nm CMOS process. A hemispheric silicon lens, rather than a hyper-hemispheric one, is used for its small sensitivity to position offset. The chip DC power is 1.7W. Each AMP is characterized independently with the bias of other AMPs turned off to entirely eliminate irrelevant radiation. The antenna radiation pattern is measured by a VDI WR-3 even-harmonic mixer (EHM) with a horn antenna at 10cm distance. Figure 17.6.4 shows the antenna pattern for the AMP at 265GHz. The average directivity of the 10 AMPs is 10.1dBi. The equivalent isotropically radiated power (EIRP) of each comb line is measured using a PM4 power meter. The total radiated power of the 10 comb lines is 5.2mW ($2f_0$=275GHz, f_D=10GHz). The average phase noise of the 10 comb lines is -102dBc/Hz at 1MHz offset. By measuring the conversion gain using an OML WR-3 frequency extender and the noise floor in the receiver mode, 14.6 to ~19.5dB SSB NF is obtained under zero AMP bias current. The calculation of NF uses the power received by the AMP antenna aperture, hence includes the antenna loss but de-embeds the performance improvement due to the beam collimation. Lastly, Fig. 17.6.5 presents a spectroscopy setup for the sensing of acetonitrile (CH_3CN) with pressure of 3Pa. One measured spectral section from 275.5 to 276GHz is shown, which agrees with the JPL molecular spectroscopy catalog [6]. An absorption line at 275.86781GHz is obtained using direct transmission as shown in Fig. 17.6.5. To further eliminate the standing wave formed inside the gas chamber, wavelength modulation with modulation frequency f_m of 50kHz, frequency deviation Δf of 240kHz is applied in one comb. The second-order derivative of the same spectrum line is then obtained by measuring the output signal at $2f_m$ from another comb, which shows a line width of 380kHz, demonstrating the absolute detection specificity. Figure 17.6.6 shows the comparison table with other state of the art systems implemented in silicon and operating above 200GHz. Through rapid combing of the spectrum, a high energy efficiency of 0.17mJ/point (1ms integration time) is achieved, demonstrating a new path for broadband sensing via parallelism.

Acknowledgements:
This work is supported by MIT Center for Integrated Circuits & Systems and TSMC University Shuttle Program. The authors acknowledge Dr. Richard Temkin at MIT and Prof. Ehsan Afshari at University of Michigan for the support of testing instruments, and Dr. Stephen Coy, Prof. Keith Nelson, Prof. Robert Field and Tingting Shi at MIT for technical discussions and assistance.

References:
[1] W. Xue et al., "A 40-to-330GHz Synthesizer-Free THz Spectroscope-on-Chip Exploiting Electromagnetic Scattering," *ISSCC*, pp. 428-429, Feb. 2016.
[2] K. Schmalz et al., "245-GHz Transmitter Array in SiGe BiCMOS for Gas Spectroscopy," *IEEE Trans. THz Sci. Technol.*, vol. 6, no. 2, pp. 318-327, Mar. 2016.
[3] N. Sharma et al., "200-280GHz CMOS RF Front-End of Transmitter for Rotational Spectroscopy," *IEEE Symp. VLSI Tech.*, pp. 329-331, June 2016.
[4] Q. Zhong et al., "A 210-to-305GHz CMOS Receiver for Rotational Spectroscopy," *ISSCC*, pp. 426-427, Feb. 2016.
[5] R. Han et al., "A SiGe Terahertz Heterodyne Imaging Transmitter with 3.3 mW Radiated Power and Fully-Integrated Phase-Locked Loop," *IEEE JSSC*, vol. 50, no. 12, pp. 2935-2947, Dec. 2015.
[6] JPL Molecular Spectroscopy, "JPL Catalog Search Form". Accessed on Sept. 2, 2016, spec.jpl.nasa.gov/ftp/pub/catalog/catform.html
[7] Z. Wang et al., "A CMOS 210-GHz Fundamental Transceiver with OOK Modulation," *IEEE JSSC*, vol. 49, no. 3, pp. 564-580, Mar. 2014.

 978-1-5090-3758-2/17/$31.00

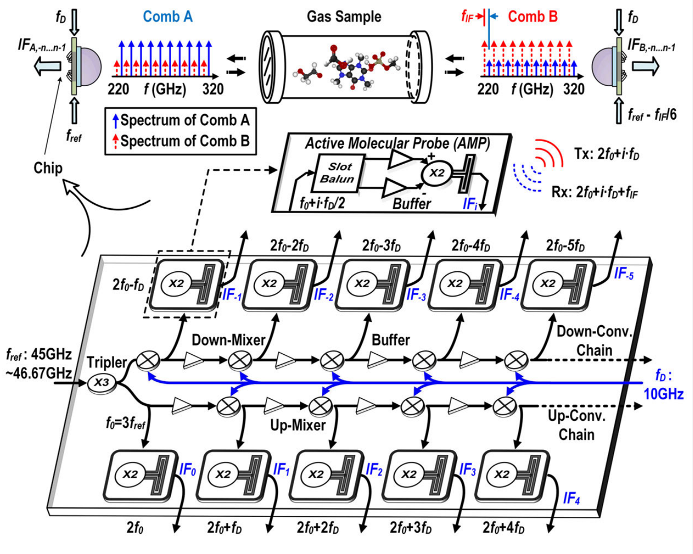

Figure 17.6.1: Dual-frequency-comb spectrometer in CMOS.

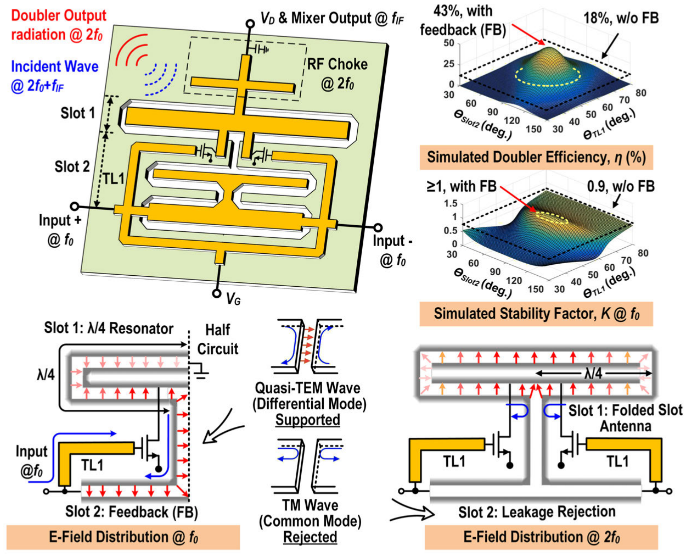

Figure 17.6.2: Active-molecular-probe (AMP) block.

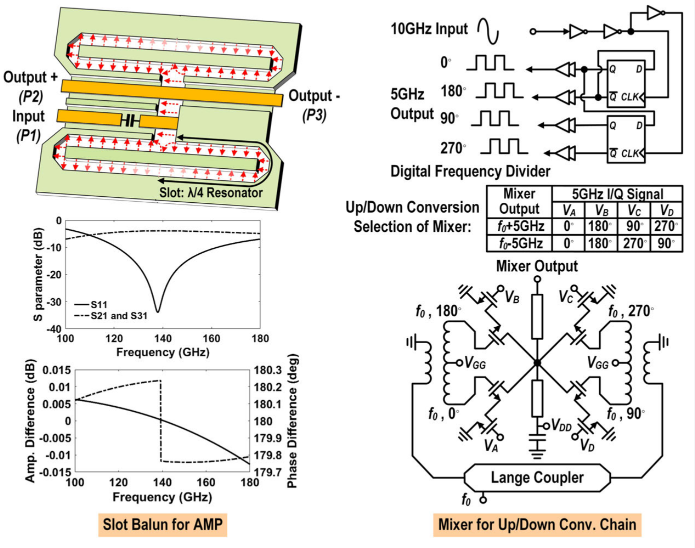

Figure 17.6.3: Slot balun and up/down-conversion mixer.

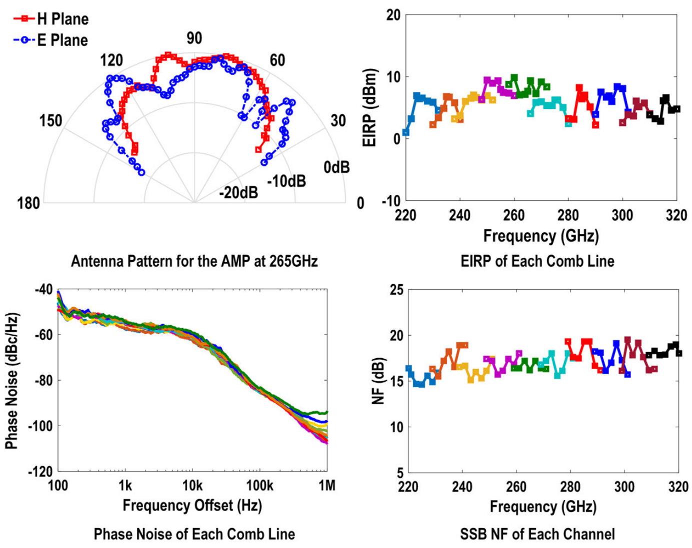

Figure 17.6.4: Measurement results of the chip.

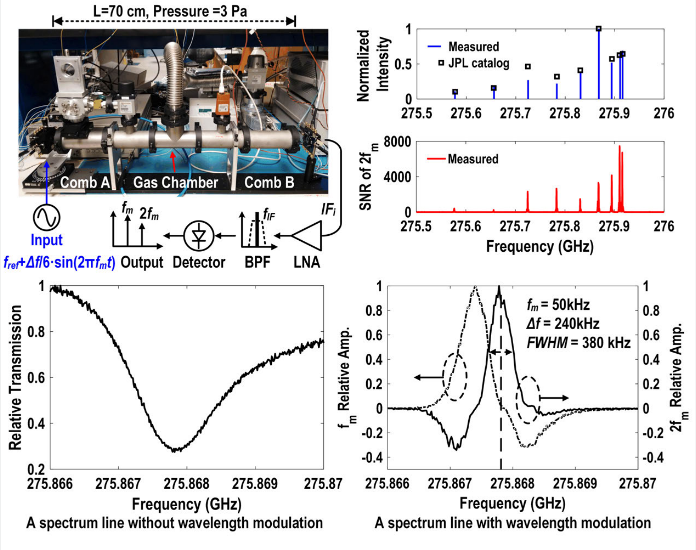

Figure 17.6.5: Spectroscopy for molecular sensing.

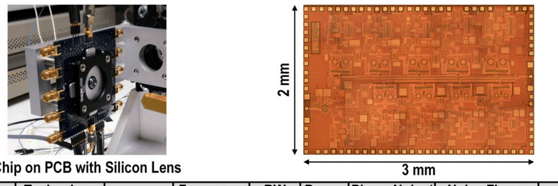

Ref.	Technology (f_{max})	Topology	Frequency (GHz)	BW (GHz)	$P_{radiated}$ (mW)	Phase Noise[1] (dBc/Hz)	Noise Figure (dB)	P_{DC} (W)
This work	65nm CMOS (250GHz)	Comb (Tx/Rx)	220~320	100	5.2	-102	14.6~19.5	1.7
[2] TST2016	0.13µm SiGe (500GHz)	Tx+Rx	245	14	4.0	-85	18	1.5+0.6 (Tx+Rx)
[7] JSSC2014	32nm CMOS (320GHz)	Tx+Rx	210	14	0.7[2]	-81	11~12[3]	0.24+0.086 (Tx+Rx)
[3] VLSI2016	65nm CMOS (N/A)	Tx	208~255	47	0.1[4]	-80	N/A	1.4
[5] JSSC2015	0.13µm SiGe (280GHz)	Tx	317	N/A	3.3	-79	N/A	0.61
[4] ISSCC2016	65nm CMOS (N/A)	Rx	210~305	95	N/A	N/A	18.4~23.5[5] (NF_{ISO}=13.9~19)	N/A

1. 1 MHz frequency offset.
2. The $P_{radiated}$ is estimated from the PA output power of 2.9 mW, and the antenna loss of 6 dB.
3. The NF of low noise amplifier in the receiver, excluding on-chip antenna loss.
4. The reported power in [3] is EIRP, not the total radiated power.
5. The overall NF (18.4~23.5 dB) =NF_{ISO}(13.9~19 dB, Isotropic Noise Figure)- (Antenna Loss (~4 dB) + Antenna Gain (-1~2 dBi)) .

Figure 17.6.6: Die micrograph and performance comparison table.

17

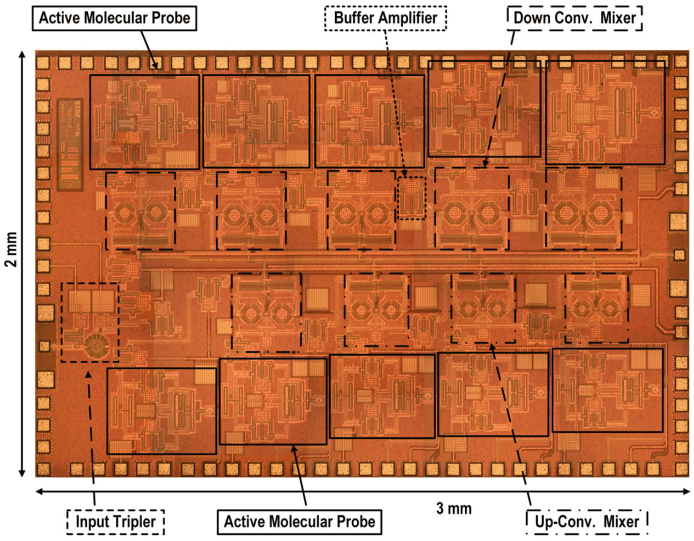

Figure 17.6.7: Die micrograph.

978-1-5090-3758-2/17/$31.00 ©2017 IEEE